Nanomechanics of silicon nanowires

Madhu Menon*
Department of Physics and Astronomy and Center for Computational Sciences, University of Kentucky, Lexington, Kentucky 40506, USA

Deepak Srivastava†
NASA Ames Research Center, Mail Stop T27-A1, Moffett Field, California 94035-1000, USA

Inna Ponomareva‡ and Leonid A. Chernozatonskii§
Institute of Biochemical Physics, Russian Academy of Sciences, Moscow 119991, Russian Federation
(Received 21 April 2004; published 20 September 2004)

The stability and elasto-mechanical properties of tetragonal and cagelike or clathrate nanowires of Si are investigated and compared using molecular dynamics simulations. Our results show that cagelike nanowires, while possessing lesser density, are able to maintain their structural integrity over a larger range of strain conditions than the tetrahedral nanowires, making them a better candidate for structural strength, chemical sensor, and electronics applications under strain conditions. This could have important technological implications.

DOI: 10.1103/PhysRevB.70.125313 PACS number(s): 61.46.+w, 68.65.−k

I. INTRODUCTION

The synthesis of silicon nanowires (Si-NW) has generated much interest in these quasi-one-dimensional materials.[1–6] They are expected to have intriguing structural, surface, electronic, and mechanical properties and can be used as model systems to demonstrate quantum size effects.[7] Experimentalists have succeeded in applying the laser ablation technique in the production of Si-NW. More recently, resistive heating activated vapor-deposition synthesis of silicon nanowires in a room-temperature chamber has also been reported.[8] All the experimental techniques used to produce nanowires have yielded Si-NW of different diameters and orientations but covered with an oxide sheet with a minimum thickness of 1–3 nm.[6] In a significant recent development, experimentalists have succeeded in removing this oxide sheet and terminating the surface with hydrogen.[9]

While the experimental results point to a crystalline core for these nanowires, whether the crystalline core is that of the bulk Si or has another arrangement of atoms is a question of great importance. It is also very likely that Si nanowires may not have uniform nature and that a particular atomic structure may depend on both the experimental conditions under which nanowires have been produced and the size of nanowire. Some possible structures for Si nanowires have been predicted recently.[10–14] In works reported in Refs. 10 and 11 nanowires consist of fullerenelike cages. The Si-NW structures proposed by Menon and Richter[10] have fourfold coordinated cores and threefold coordinated surfaces with one of the most stable reconstructions of bulk Si. Such reconstruction is of great importance since it provides a reduction in the surface energy that can be relatively high for quasi-one-dimensional structures. In the work of Li *et al.*,[13] Si clusters of different sizes were used as subunits for nanowire structures. In this work the thinnest nanowire structure consisting of uncapped trigonal prism was proposed and stability of wires consisting of multicoordinated Si atoms was investigated. There is one important fact that serves in favor of such models: in order to develop the one-dimensional structure in vapor phase the nanowire structure should be essentially anisotropic.[11] Recently, Zhao *et al.*,[14] have compared the energetics of formation of Si-NW with crystalline and polycrystalline cores and concluded that for very thin (1–3 nm) nanowires polycrystalline is a lower energy structure than the single crystal structure observed in experiments. It should be noted that polycrystalline structure is essentially tetrahedral in nature with stacking fault type grain boundaries as defects.

These works suggest that the Si-NW core can possess either tetrahedral or cagelike features. Because of their tremendous potential in nanotechnology applications, their properties are of great importance for researchers working in the area of Si-NW. Despite the increasing volume of work on Si-NW, to the best of our knowledge, currently no information is available (theoretical or experimental) on their elasto-mechanical properties. A rigorous theoretical investigation of the structural, energetic, and mechanical properties of the Si-NW is, therefore, necessary and timely.

In this work, we investigate structural, energetic, and mechanical properties of Si-NW ($\approx$4 nm diameter, within the range of experimentally produced wires[9]) for a comparison between tetrahedral and hollow cage (clathrate) like configurations. The hollow cage or clathratelike structures for a crystalline configuration of Si nanowires[10] are feasible because for bulk lattice structures, the clathrates are very close in energies to the diamond lattice (tetrahedral) structure; the lowest energy configuration for Si. The cagelike structures for Si-NW could be of lower density and of similar mechanical characteristics and different electronic properties, and hence could be useful for nano materials and electronics applications.

We investigate the structure, stability, and mechanical properties of tetrahedral and cagelike Si-NW using molecular dynamics and energetics simulations with the Stillinger-

TABLE I. Comparison of cohesive energies and elastic constants obtained using the SW potential for tetrahedral and cagelike Si-NW along with the corresponding bulk values. The Young's modulus for bulk tetrahedral solid was computed for the (111) direction. The experimental values quoted from Ref. 22 are indicated in brackets for comparison.

Structure	Cohesive energy (eV/atom)	Density (g/cm^3)	Young's modulus (GPa)	Bending stiffness (eV^*m)	Poisson's ratio
Tetrahedral nanowire	4.16	2.49	147.3	12.2×10^{-6}	0.162
Cagelike nanowire	4.11	2.11	94.43	8.5×10^{-6}	0.107
Tetrahedral bulk	4.34	2.33 (2.33)	148.89 (160)		0.25 (0.27)
Clathrate bulk	4.29	2.05	105.89		0.201

Weber (SW) many-body potential[15] for Si-Si interactions. The empirical SW interatomic potential consists of two- and three-body interaction terms and was originally fitted to describe the crystalline and liquid silicon phases. This potential consists of sums of two- and three-body interaction contributions. The two-body potential describes the formation of a chemical bond between two atoms. The three-body potential favors structures in which the angles between two bonds made by the same atom are close to the tetrahedral angle. The interaction range of the potential is governed by parameters that place the interaction cutoff at approximately 3.77 Å, which is between the first and second-neighbor distances for crystalline Si. The SW potential has been used in the study of molten Si (Ref. 15) as well as surfaces of crystalline Si.[16] The SW potential has also been adopted for the study of germanium and found to give an excellent structural representation of amorphous solid Ge as well as crystalline Ge and give good results for several thermodynamic properties.[17]

The static energetics and temperature dependent dynamic stability behavior of Si-NW of $\approx 3-4$ nm diameter are investigated first and compared for tetrahedral (T) and cagelike (C) crystalline structures. The cagelike Si-NW used in this work is carved out from a Si clathrate structure consisting of a simple cubic (sc) lattice with a 46 atom basis.[18] This is known to be one of the most stable clathrate forms for Si. The cohesive energy of this clathrate structure is obtained to be 4.29 eV/atom using the SW potential. The value for diamond structure, by comparison, is 4.34 eV/atom. In the 3–5 nm diameter range, the energies of the formation of T and C type Si-NW should be comparable to each other.

II. RESULTS

The two types of S-NW considered in this work consist of T and C type nanowires of lengths 7.3 nm (5184 atoms) and 11.2 nm (6702 atoms), respectively. They are both relaxed without any symmetry constraints using the SW potential. For the relaxed T and C type Si-NW, the bond lengths near the center of the core are comparable to the bulk Si tetragonal and clathrate values, whereas the values for the surface atoms are closer to the corresponding bulk surface atoms values, respectively. The main point is that the cohesive energies for T and C type Si-NW obtained using the SW potential are within 0.05 eV (see Table I) of each other, so it is possible that C type of nanowires could be made in experiments. The densities of the T and C type nanowires were also computed and listed in Table I. As expected, the C type nanowire has smaller density than the T type nanowire, since the cage type structure is more open as compared to that of the more tightly packed diamondlike structure. Interestingly, the densities of fully relaxed T and C type Si-NW are larger than their corresponding bulk values. This is due to the surface formation in the nanowire structures which causes a small inward compression of the Si layers in both T and C configurations. Such compressions are well known in silicon surface formation studies and found to extend a few layers deep from the surface. The elasto-mechanical characteristics of the two types of nanowires are computed and discussed next.

A. Deformation under compressive and tensile strains

For determining the elastomechanical properties, the T and C type nanowires are strained dynamically under axial compression and tension. The Young's modulus and bending

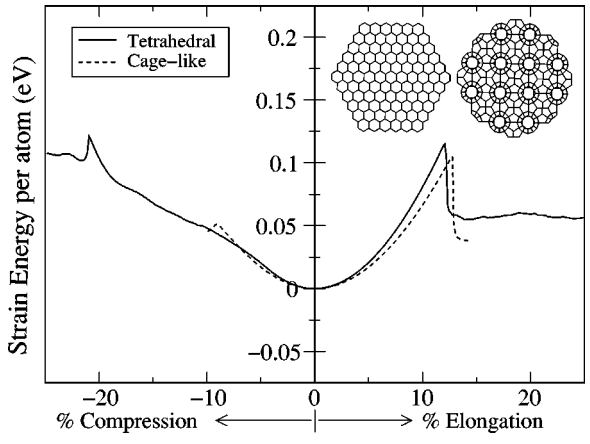

FIG. 1. The strain energy as a function of % strain for compression/elongation of tetrahedral and cagelike Si-NW. The inset shows cross sections of tetrahedral (left) and cagelike (right) nanowires used in the calculations. The plot is used in obtaining the Young's modulus.

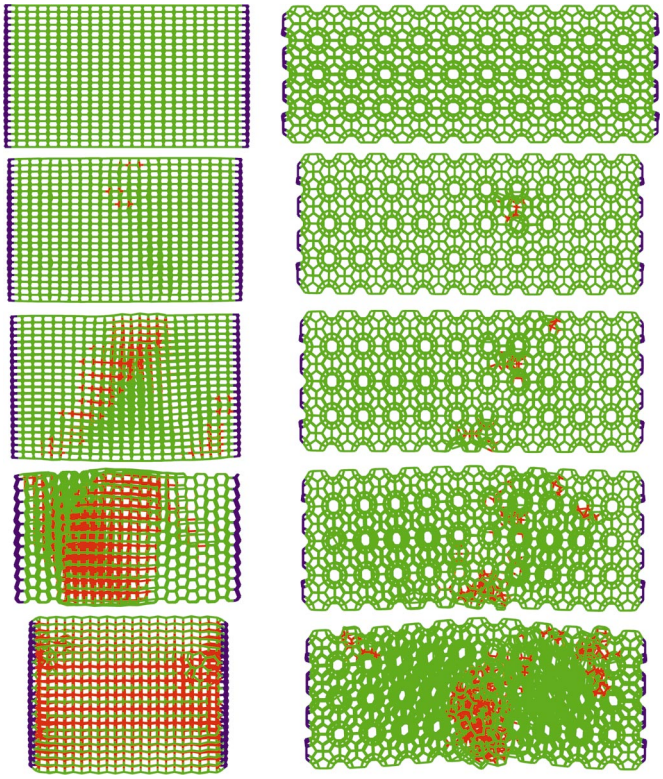

FIG. 2. (Color) Five stages (top to bottom) of strained configurations of tetrahedral (left) and cagelike (right) Si-NW under uniaxial compression. The atoms shown in red have fivefold or more coordination. The atoms at both ends are shown in blue and are held fixed throughout. The compression values for the tetrahedral wire are, respectively, 0%, 6.4%, 8.7%, 11.0%, and 20.93% (beginning of plastic collapse). The values for the cagelike wire are, respectively, 0%, 7.96%, 8.67%, 9.03% (beginning of plastic collapse), and 9.57%.

stiffness under different stresses and the mechanism to failure near elastic limit were investigated. Briefly, compression,[19] and stretching[20] of the two types of nanowires are achieved similarly to the nanomechanics of carbon nanotubes investigated in detail recently.[19–21] A few layers of edge atoms of the nanowire are held by the extra constraint forces and moved inward or outward to simulate dynamic compression and tension of the nanowires, respectively. For compression and stretching the constrained edge atom layers are moved in steps of 0.13% strain for T type and 0.09% for C type Si-NW, respectively, and the system is then dynamically relaxed as the axial strain builds up. For each loading step of our simulations the nanowires were heated up to the melting point of bulk tetrahedral Si to verify the stability.

The changes in the total energy with respect to the total energy of the initial strain free configuration reflects the strain energy as a function of strain and are shown in Fig. 1. The inset shows cross sections of the two nanowires. The Young's modulus for compression and tension as defined in Ref. 21 was computed for small strains and listed in Table I. In all cases, we find that for small axial strain the Young's modulus of the T type nanowire is about 56% more than the axial Young's modulus of the C type nanowire. This is

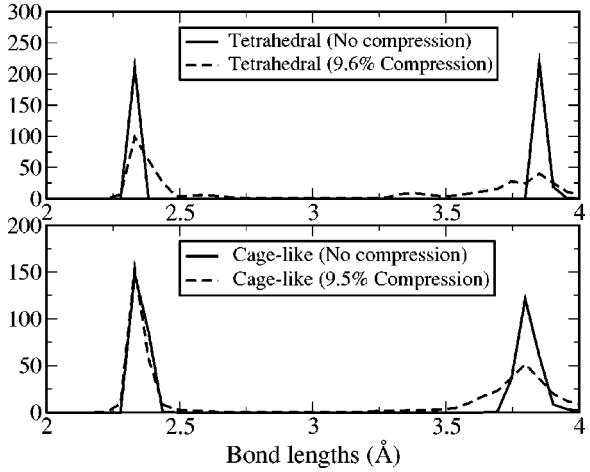

FIG. 3. The radial distribution function (RDF) for the T and C type of Si-NW for approximately the same value of compression. As the figure shows, the C type nanowire provides better resistance to the structural changes.

expected because for nanowires of similar cross sections, the diamond (T) type lattice structure is supposed to be the strongest and stiffest. However, the difference with the more open cage (C) type nanowire structure is not large when comparing the normalized (modulus/density) in the two cases (59.16 vs 47.75 in units of $\mathrm{GPa/g/cm^3}$, see Table I).

The changes in the structure in the form of changes in the coordination number or number of nearest neighbors, as the T and C type nanowires are compressed are shown in Fig. 2. Under compression the first appearance of fivefold coordinated atoms (shown in red) occurs at 4.16% strain in the middle region of the T type nanowire. The formation of fivefold coordinated atoms accelerates with the increase in compression and at 5.8% strain value the beginning of greater than fivefold coordination is seen. It is worth noting that for this strain value the number of fivefold coordinated atoms is about 5% of the total, increasing to about 50% for a strain value of 12.6%. The multicoordinated atoms first form in the middle of the wire and spread throughout evenly. There is a noticeable increase in the diameter of the nanowire on compression. This new configuration of wire is unstable and buckles when allowed to relax without any constraints. At 17% strain value all atoms (except those on the surface as well as atoms held fixed at both ends) have coordination in excess of four. Buckling of the wire occurs at 20.93% strain. It corresponds to the breakdown of the metastable configuration from both ends of the nanowire. For compression the elastic limit is concurrant with the appearance of fivefold coordinated atoms and is found to occur at 4.3% strain.[23] For defining the elastic limit we heated the nanowire at every strain step up to the melting point after removing the constraints at both ends. This was followed by a slow cooling. Strain value for which the unconstrained nanowire did not return to its original form was taken to be the elastic limit.

In the case of C type nanowire fivefold coordinated atoms make their first appearance at 7.96% strain value (see Fig. 2). The elastic limit for the C type nanowire is found to be

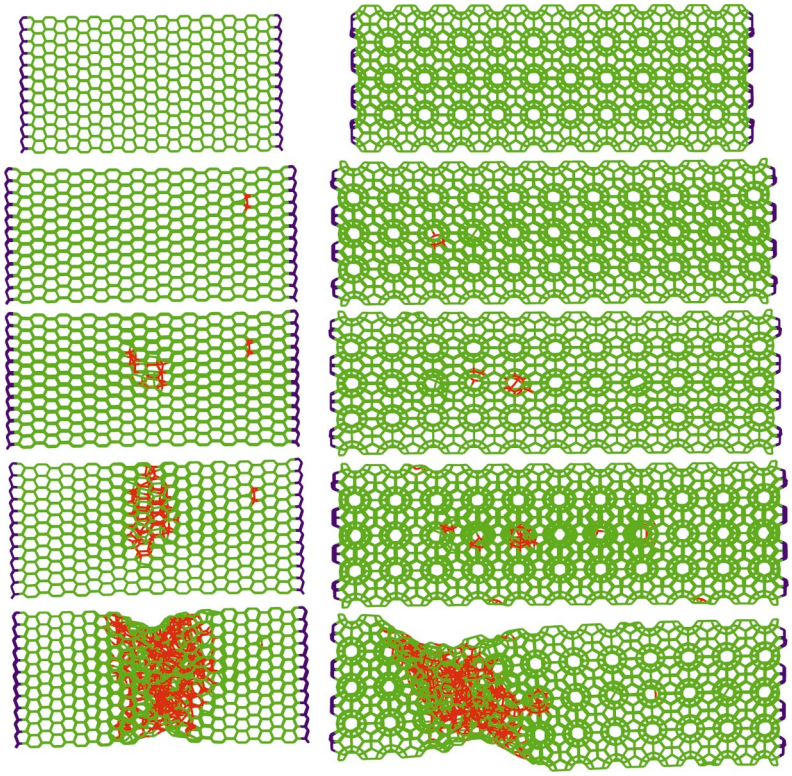

FIG. 4. (Color) Five stages (top to bottom) of elongation of a tetrahedral (left) and a cagelike (right) Si nanowire under tensile strain. The atoms shown in red have fivefold or more coordination. The atoms at both ends are shown in blue and are held fixed throughout. The elongation values for the tetrahedral wire are, respectively, 0%, 11.4%, 11.9% (beginning of collapse), 12.1%, and 12.3%. The values for the cagelike wire are, respectively, 0%, 10.28%, 12.16%, and 12.7% (beginning of collapse), and 12.88%.

8.05%. At 8.67% strain value there are three localized regions with multicoordinated atoms. These regions are located near the wire surface and grow rapidly as the compression is increased. At 9.03% strain the fraction of the multicoordinated atoms is 1.8%. It is worth noting that for the same value of strain the fraction of multicoordinated atoms in the T type wire is 28.5%. Buckling occurs at the center of the wire at the strain value of 9.03% for the C type nanowire.

The radial distribution function (RDF) shown in Fig. 3 illustrates the striking differences in the structural changes in the T and C types of nanowires for similar compression values. The peak at the nearest neighbor distance is considerably less affected for the C type nanowire indicating better structural integrity under compression.

Under tensile strain (Fig. 4), fivefold coordinated atoms first appear at 10.26% strain value for the T type nanowire. At 11.5% strain a second island of multicoordinated atoms appear. On further streching buckling occurs at 11.92% strain. Elastic limit coincides with the onset of multicoordinated atoms for the T type nanowire. For the C type nanowire, fivefold atoms make their appearance at 9.03% strain. The elastic limit is reached at 11.8% strain and buckling at 12.7%.

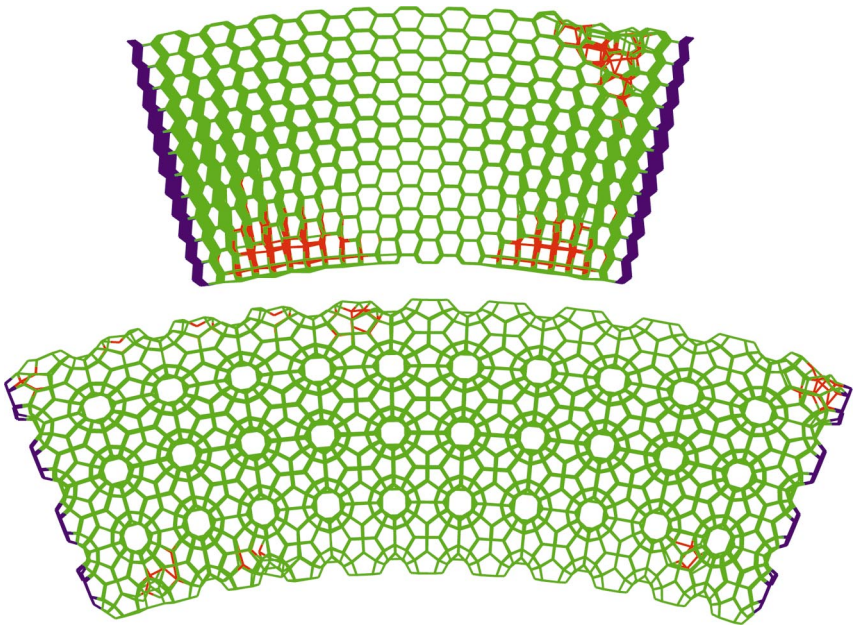

FIG. 5. (Color) Bent configurations for T (top) and C (bottom) type Si-NW for angles 0.53 rad and 0.80 rad, respectively.

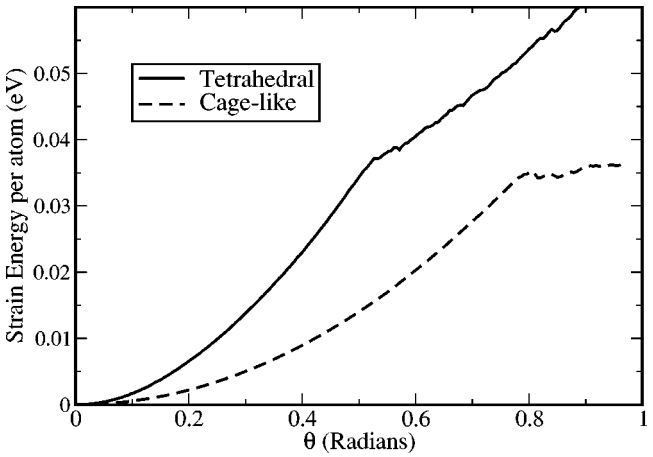

FIG. 6. The changes in the total energy with respect to the total energy of the initial strain free configuration as a function of angle under bending strain for tetrahedral and a cagelike Si-NW.

These results point to a significant advantage for the C type nanowires over the T type under strain conditions. Note that the onset of the plasticity via the irreversible formation of fivefold coordinated Si atom defects under compression occurs at a much smaller value of strain (4.16%) in the T type wire as compared to the C type wire (8.05%). It is expected that the structural, chemical, and electronic characteristics of the nanowires will change significantly after the formation of fivefold coordinated Si atom defects. The C type nanowires are able to resist the formation of such defects and change in the initial characteristics of the nanowire for higher axial compression values than the T type nanowires. Under compression, the density normalized elastic limit of the C type nanowire is higher by a factor of 2.21 as compared to the density normalized elastic limit of the T type nanowire.

B. Deformation under bending strain

We next investigate the bending stiffness under different stress and the mechanism to failure near elastic limit. Bending of the two types of nanowires are achieved similarly to the nanomechanics of carbon nanotubes investigated in detail recently.[21] A few layers of edge atoms of the nanowires are held by the extra constraint forces and moved in an arc to simulate dynamic bending of the nanowires. The bending strain was incremented in steps of 0.005 radians with a full dynamical relaxation of about 14500 MD steps between each successive step. Figure 5 shows bent configurations for T and C type nanowires for angles 0.53 rad and 0.80 rad, respectively. For each loading step of our simulations the nanowires were heated upto the melting point of bulk tetrahedral Si to verify the stability. The bending stiffness as defined in Ref. 21 was computed for small strains and listed in Table I. Figure 6 shows a plot of strain energy as a function of angle.

For the T type nanowire, the onset of fivefold coordinated atoms occurs at 0.21 rad. Five-fold coordinated atoms appear almost symmetrically with respect to the ends of nanowires. In going from a bend of 0.21 rad to 0.25 rad, the total number of fivefold atoms changes only slightly but they move from the ends of the nanowire towards its center. In the area of maximum stress (bending point) there is a rearrangement of atoms so that the tetrahedral configuration in this region is no longer regular. There is also a change in the Si-Si bond lengths. The Si-Si bonds in this region experience a greater contraction compared to the surrounding. The Si-Si bonds on the outer region undergo elongation on bending. At a bending angle of 0.26 rad there is a significant increase in the number of fivefold coordinated atoms. Formation of multicoordinated atoms result in strain release in the structure so that in the undamaged areas (areas without multicoordinated atoms) both bond length and tetrahedral angle are close to the equilibrium values. The number of fivefold coordinated atoms continue to increase as the bending angle is increased from 0.26 rad. The number of fivefold coordinated atoms, originally formed at the ends, begin to move towards the center. This process continues till the number of such atoms reaches 3.4% of the total number of atoms. At 0.49 rad atoms with more than fivefold coordination begin to appear at the side of the wire that is elongated on bending. The region containing these atoms give indication of the beginning of buckling. This process continues until the bending angle of 0.53 rad is reached when buckling occurs. Bending strain elastic limit coincides with the onset of the fivefold coordinated atoms (0.21 rad).

For the C type nanowire, both the onset of fivefold as well as greater than fivefold coordinated atoms occurs for the same value of the bending angle (0.57 rad). This is strikingly different from the case of the T type wire. The defect formation process for the C type wire in the form of multicoordinated atoms is also significantly different from the T type wire. Such defects appear at the elongated side of the wire first. They are relatively stable, remaining at the same position while their number also remains the same until a bending angle of 0.66 rad is reached. Another interesting difference worth noting is that the undamaged regions remains almost perfectly regular despite changes in the bond lengths and the bond angles. At a bending angle of 0.67 rad, fivefold coordinated atoms make their first appearance in the contracted region of the wire. When buckling finally occurs, it happens symmetrically from both sides. Elastic limit for the C type wire is reached at a bending angle of 0.65 rad. This is more than three times the corresponding value for the T type wire indicating greater structural integrity for the C type wire under bending strain. Since many practical applications of nanowires are based on their ability to restore to their original shape after loading, the important advantage of the C type wire is evident.

III. SUMMARY

In summary, we have investigated and compared the structural and mechanical properties of tetrahedral (T) and cagelike (C) Si-NW. Our results show that C type nanowires, while possessing lesser density, are nevertheless able to maintain their structural integrity over a larger range of strain

conditions than the T type nanowires. This makes them a better candidate for structural strength, chemical sensor, and electronics applications under strain conditions. Unlike the T type nanowires, many different C type nanowires are possible since a large variety of underlying clathrate crystal structures exists. Synthesis of C type nanowire with the largest density normalized elastic limit value will, therefore, have important technological implications.

ACKNOWLEDGMENTS

The present work is supported through grants by NSF (No. ITR-0221916), DOE (No. 00-63857), NASA (No. 02-465679) and KSTC (No. 03-66986). D.S. acknowledges support from NASA (Contract No. NAS2-03144 to UARC). L.C. and I.P. acknowledge support from the Russian program "Topical directions in condensed matter physics."

*Electronic address: super250@pop.uky.edu
†Electronic address: deepak@nas.nasa.gov
‡Electronic address: iponomar@sky.chph.ras.ru
§Electronic address: cherno@sky.chph.ras.ru

[1] T. Ono, H. Saitoh, and M. Esashi, Appl. Phys. Lett. **70**, 1852 (1997).
[2] D. P. Yu, C. S. Lee, I. Bello, X. S. Sun, Y. H. Tang, G. Zhou, Z. Bai, Z. Zhang, and S. Q. Feng, Solid State Commun. **105**, 403 (1998).
[3] N. Wang, Y. H. Tang, Y. F. Zhang, D. P. Yu, and S. T. L. C. S. Lee, and I. Bello, Chem. Phys. Lett. **283**, 368 (1998).
[4] N. Wang, Y. H. Tang, Y. F. Zhang, C. S. Lee, and S. T. Lee, Phys. Rev. B **58**, R16 024 (1998).
[5] A. M. Morales and C. M. Lieber, Science **279**, 208 (1998).
[6] Y. F. Zhang, L. S. Liao, W. H. Chan, S. T. Lee, R. Sammynaiken, and T. K. Sham, Phys. Rev. B **61**, 8298 (2000).
[7] R. Wang, G. Zhou, Y. Liu, S. Pan, H. Zhang, D. Yu, and Z. Zhang, Phys. Rev. B **61**, 16 827 (2000).
[8] O. Englander, D. Christensen, and L. Lin, Appl. Phys. Lett. **82**, 4797 (2003).
[9] D. D. D. Ma, C. S. Lee, F. C. K. Au, S. Y. Tong, and S. T. Lee, Science **299**, 1874 (2003).
[10] M. Menon and E. Richter, Phys. Rev. Lett. **83**, 792 (1999).
[11] B. Marsen and K. Sattler, Phys. Rev. B **60**, 11 593 (1999).
[12] U. Landman, R. N. Barnett, A. G. Scherbakov, and P. Avouris, Phys. Rev. Lett. **85**, 1958 (2000).
[13] B. Xing Li, P. Lin Cao, R. Q. Zhang, and S. T. Lee, Phys. Rev. B **65**, 125305 (2002).
[14] Y. Zhao and B. I. Yakobson, Phys. Rev. Lett. **91**, 035501 (2003).
[15] F. Stillinger and T. Weber, Phys. Rev. B **31**, 5262 (1985).
[16] F. F. Abraham and I. P. Batra, Surf. Sci. **163**, L752 (1985).
[17] K. Ding and H. C. Andersen, Phys. Rev. B **34**, 6987 (1986).
[18] M. Menon, E. Richter, and K. R. Subbaswamy, Phys. Rev. B **56**, 12 290 (1997).
[19] D. Srivastava, M. Menon, and K. Cho, Phys. Rev. Lett. **83**, 2973 (1999).
[20] C. Wei, D. Srivastava, and K. Cho, Phys. Rev. B **67**, 115407 (2003).
[21] D. Srivastava, C. Wei, and K. Cho, Appl. Mech. Rev. **56**, 215 (2003).
[22] P. Hess, Appl. Surf. Sci. **106**, 429 (1996).
[23] Note that the formation of some multicoordinated atoms is reversible, i.e., they can become fourfold coordinated when allowed to relax by removing all constraints. This is the case when the onset of multicoordinated atoms do not coincide with the elastic limit. Placticity, on the other hand, is determined by an irreversible formation of such atoms.